A High Performance RST Controller for on Board Battery Charger

S. LACROIX, Student Member, IEEE, M. HILAIRET, Member, IEEE, E. LABOURE
Laboratoire de Génie Electrique de Paris (LGEP)/ SPEE-Labs ;
CNRS UMR8507; SUPELEC; Université Pierre et Marie Curie P6; Université Paris-Sud 11;
11, rue Joliot Curie, Plateau de Moulon F91192 Gif Sur Yvette Cedex
(samantha.lacroix, mickael.hilairet, eric.laboure)@lgep.supelec.fr

***Abstract*- Controllers for on board battery charger of Electric Vehicles are studied. To ensure the regulation of the grid currents of PWM inverters different kind of RST controllers are presented. Pole placement controllers allowing the cancellation of steady state errors in response to polynomial reference signals has been introduced few years ago. This paper proposed to compare different RST controllers in terms of performances, such as stability, robustness and dynamic, when sine wave references are used. These controllers are applied to an on board battery charger which uses an electrical machine as filtering inductances.**

I. Introduction

An on board battery charger is an interesting solution for the development of Electric Vehicles (EV). For such applications, it is important to optimize the whole system to address environmental and economic issues. From this idea, several battery charger topologies was proposed and studied. These new technological solutions have many advantages over the more conventional one using off-board chargers [1]-[2]. This solution has the drawback of being very expensive because of the need to implement a large number of equipment and do not offer the possibility of charging anywhere.

To overcome these problems, the idea of integrating the charger to the vehicle and thus reduce the numbers of components by using them for several functions grew up. Some examples are presented in [2]-[6]. In [2]-[4], the motor driving inverter and the motor windings used as filtering inductors are connected to a single phase grid and represent the elements of a battery charger. In [5] and [6], the authors also used the motor, but as an isolated three-phase transformer. The specificity of this particular topology is due to the existence of a rotating magnetic field. This implies that the electric motor rotates during batteries charging.

The topology proposed in this paper is based on this principle and reduces the number of power electronics devices using the same components for different functions. Fig. 1 represents the power train of the studied EV. In charging mode, two ways to connect the grid are possible namely a single-phase or three-phase connection via the electric machine. The overall problem is presented in [7]-[8]. In [9] the traction mode operation is described and information about charging mode are given in [10]-[11]. In this paper, we study the control of the converter in the single-phase charging mode configuration.

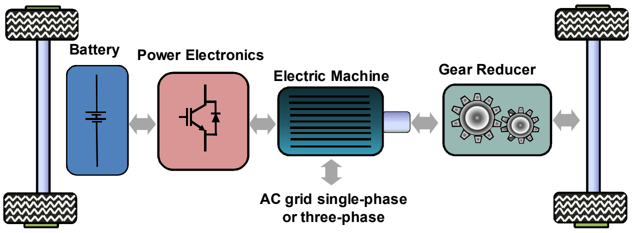

Fig. 1. Propulsion and recharge Electric Vehicle system

To control the power converter, a linear controller, based on the robust pole placement method (RST) is proposed. The design is based on the resolution of a Diophantine equation. It allows the rejection of low-frequency disturbances for polynomial reference signals regardless of the order of this polynomial, and also ensures a unity static gain for the closed-loop [12]-[13]. Design of the polynomial RST controller is recalled in [14]-[19]. The tuning parameters of this controller are easily computed from the system expression. Nevertheless this controller considers only constant references. In case of variations of the references, there is a static error this means that the system responses do not reach the references. A RST controller designed for polynomial (ramp) and sinusoidal references are respectively developed in [20] and [13], [21]. This design method gives a near zero error in steady state.

This paper presents the design of a RST controller for an on board battery charger in order to regulate the currents drawn on the grid and minimize the static errors. In the first part, the power converter topology and state model are introduced and the particularities of the structure are pointed out. In order to consider these elements and manage easily the compromise between dynamic performances and robustness, the behavior of polynomial RST controllers are studied. Section III recalls the design of each controller and results are shown in part IV. Comparisons between regular RST, RST with polynomial reference signal and RST with sinusoidal reference are done. Then, section V provides a conclusion and a discussion about future works.

978-1-61284-972-0/11/$26.00 ©2011 IEEE

II. DESCRIPTION OF THE BATTERY CHARGER

The battery charger presented here is a single phase charger but it can also be used in a three-phase configuration. More details about the context and the structure of the power converter are available in [7]-[11]. The topology principle leads to optimize the use of power converter and electrical motor by reducing cost and number of power devices.

In single-phase charging mode, the power converter is equivalent to two interleaved PFC (Power Factor Corrector). Fig. 2 shows the power circuit corresponding to the proposed converter, where each phase of the AC grid is connected to two parallel PFC converters. This connection is realized through the midpoint of each winding of the electric al motor. The aim is to ensure the same current in each half windings of a given phase, to eliminate the rotating magnetic field components at the stator level.

By controlling the two PFC converters, DC link voltage U_{dc} can be maintained at a defined constant value in order to adapt the active power to the load. Control of AC currents grid (i_a, i_b, i_c, i_d) by appropriate sine wave references provides a unity power factor.

Moreover, using the winding inductances of the electrical machine to filter currents is conceptually very interesting but the control is different from a classical boost converter operating in a PFC mode. Indeed the state space model of the system given in (1)-(5) shows some specificities due to mutual inductances of the electrical machine and variations of inductances with the rotor position.

$$\dot{\boldsymbol{X}} = \boldsymbol{A_c X} + \boldsymbol{B_c}(\boldsymbol{X})\boldsymbol{u} + \boldsymbol{D_c} \tag{1}$$

$$\boldsymbol{Y} = \boldsymbol{CX}, \quad (\boldsymbol{C} = \mathbf{I_4}) \tag{2}$$

with,

$$\boldsymbol{X} = [i_a\ i_b\ i_c\ i_d\ U_{dc}]^t \tag{3}$$

$$\boldsymbol{A_c} = -R_s \begin{bmatrix} Y_1 & Y_{12} & Y_{13} & Y_{14} & 0 \\ Y_{12} & Y_1 & Y_{14} & Y_{13} & 0 \\ Y_{13} & Y_{14} & Y_2 & Y_{34} & 0 \\ Y_{14} & Y_{13} & Y_{34} & Y_2 & 0 \\ 0 & 0 & 0 & 0 & 1/\mathrm{r_{load}} R_s \mathrm{C} \end{bmatrix} \tag{4}$$

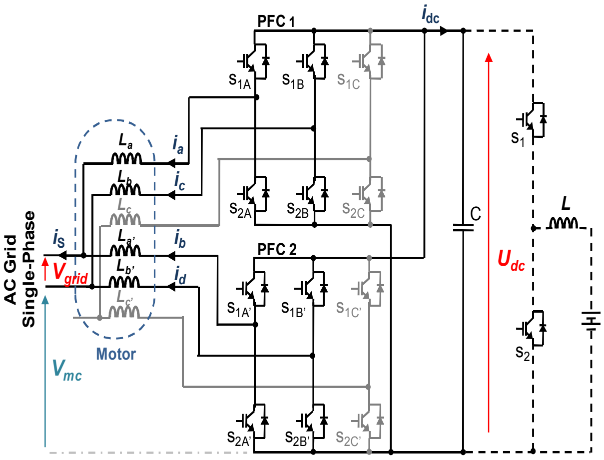

Fig.2. Equivalent circuit in single-phase charging mode

and

$$\boldsymbol{B_c} = \begin{bmatrix} Y_1 & Y_{12} & Y_{13} & Y_{14} & 0 \\ Y_{12} & Y_1 & Y_{14} & Y_{13} & 0 \\ Y_{13} & Y_{14} & Y_2 & Y_{34} & 0 \\ Y_{14} & Y_{13} & Y_{34} & Y_2 & 0 \\ 0 & 0 & 0 & 0 & 1/\mathrm{C} \end{bmatrix} \begin{bmatrix} \mathrm{U_{dc}} & 0 & 0 & 0 \\ 0 & \mathrm{U_{dc}} & 0 & 0 \\ 0 & 0 & \mathrm{U_{dc}} & 0 \\ 0 & 0 & 0 & \mathrm{U_{dc}} \\ -i_\mathrm{a} & -i_\mathrm{b} & -i_\mathrm{c} & -i_\mathrm{d} \end{bmatrix} \tag{5}$$

$$\boldsymbol{D_c} = -\boldsymbol{V_{grid}} \begin{bmatrix} 1/2 \\ 1/2 \\ -1/2 \\ -1/2 \end{bmatrix} - \boldsymbol{V_{cm}} \begin{bmatrix} 1 \\ 1 \\ 1 \\ 1 \end{bmatrix}$$

where $\boldsymbol{X}$, represents the state vector, $\boldsymbol{u}$ is the control vector, i.e. the four half bridge duty cycles, equal to $[d_1\ d_2\ d_3\ d_4]^t$. $\boldsymbol{D_c}$ is a measurable disturbance to be compensated by the controller. Terms $\boldsymbol{Y_k}$ used are not the inductances but the admittances. The control matrix $\boldsymbol{B_c}$ is multiply by control vector $\boldsymbol{u}$, where each duty cycles d_k has an influence on the state vector. The system is coupled and non-linear.

From these elements, i.e. the mathematical non-linearity, the coupling of the system and the variations associated with the rotor position, the idea is to develop a robust controller, which will be able to regulate the currents and the DC-bus voltage regardless the rotor position and uncertainties on parameter values.

This has been achieved using a RST controller. Different RST controllers have been tested on this complex system. In order to compute these controllers, we were led to the following hypothesis: the mutual inductances of the electric machine are assumed negligible. AC grid voltage V_{grid} and common voltage V_{cm} are considered like measurable perturbations and the DC link voltage is assumed nearly constant according to the currents dynamic. Therefore, the system is represented by 5 first order transfers functions.

$$\frac{i_a}{d_1} = \frac{U_{dc}}{(L_1 s + R_s)} - \frac{V_{grid}}{2} - V_{cm} \tag{6}$$

$$\frac{i_b}{d_2} = \frac{U_{dc}}{(L_1 s + R_s)} - \frac{V_{grid}}{2} - V_{cm} \tag{7}$$

$$\frac{i_c}{d_3} = \frac{U_{dc}}{(L_2 s + R_s)} + \frac{V_{grid}}{2} - V_{cm} \tag{8}$$

$$\frac{i_d}{d_4} = \frac{U_{dc}}{(L_2 s + R_s)} + \frac{V_{grid}}{2} - V_{cm} \tag{9}$$

$$\frac{U_{dc}}{i_{dc}} = \frac{r_{load}}{(1 + r_{load} C s)} \tag{10}$$

with, $$i_{dc} = -\boldsymbol{i}^t\boldsymbol{u} = -(i_a d_1 + i_b d_2 + i_c d_3 + i_d d_4) \tag{11}$$

where i_{dc} is the DC link current.

III. CONTROLLERS SYNTHESIS

In this section, three different linear controllers for the currents control are presented. The polynomial RST is first tested and compared to RST with polynomial reference signals and RST with sinusoidal reference signals.

The simplifications mentioned above allow considering four first order transfer functions:

$$H(s) = \frac{K}{1+\tau s} \tag{12}$$

and the corresponding discretized form with a sampling period T_s is :

$$H(z^{-1}) = K\frac{(1-a)z^{-1}}{1-az^{-1}} = \frac{B(z^{-1})}{A(z^{-1})} \tag{13}$$

with $a = e^{-Ts/\tau}$. In Equ. (13) B/A is the global transfer function.

A. Polynomial RST

The polynomial RST controller seems to provide an alternative solution better to PI controllers. Indeed it allows a compromise between dynamic and precision. It is based on the pole placement theory, and it is possible to impose poles in closed-loop and to carry out separately the objectives of tracking and regulation.

The block diagram of a regular system with RST controller is presented in Fig. 3, where $B(z^{-1})/A(z^{-1})$ represents the open-loop transfer function. The closed-loop transfer function is given by:

$$y = \frac{BT}{AS+BR}y_c + \frac{S}{AS+BR}d \tag{14}$$

where, y is the output, y_c the reference and d the disturbance. Polynomials $R(z^{-1})$ and $S(z^{-1})$ are obtained by a pole placement strategy and are solutions of the Diophantine equation:

$$A(z^{-1})S(z^{-1}) + B(z^{-1})R(z^{-1}) = D(z^{-1}) \tag{15}$$

Degrees of S and R depend on the type of controller: proper or strictly proper. The choice of a strictly proper controller is done. In fact, this latter is better suited for high frequency noise rejection. So, if the degree of polynomial A is equal to n:

$$\begin{aligned} deg(S) &= deg(A) + 1 \\ deg(R) &= deg(A) \\ deg(D) &= 2n + 1 \end{aligned}$$

Since deg (A) is equal to one:

$$\begin{aligned} R(z^{-1}) &= r_1 z^{-1} + r_0 \\ S(z^{-1}) &= (1 - z^{-1})(s_1' z^{-1} + s_0') \end{aligned}$$

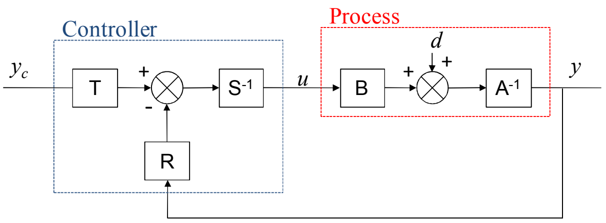

Fig. 3. System with RST controller.

Then, the poles of the closed-loop are imposed in the discrete plan, such as:

$$\begin{aligned} z_{1,2} &= e^{(-\xi_0\omega_0 \pm j\omega_0\sqrt{1-\xi_0{}^2})T_s} \\ z_3 &= e^{-\omega_0 T_s} \end{aligned}$$

that leads to the polynomial $D(z^{-1})$. From this, the coefficients of polynomials R and S are identified.

To protect the components, the outputs of some controllers can be saturated. To ensure a proper behavior of this saturation, an anti-windup function is implemented, as shown in Fig. 4.

Polynomial $T(z^{-1})$ is a free tuning parameter with two constraints: (i) the transfer BT/D is at least proper, (ii) $T(1) = R(1)$ in order to ensure a unity gain of the transfer y/y_c at steady state. Polynomial T is defined as follow:

$$T(z^{-1}) = \frac{R(1)}{F(1)}F(z^{-1}) = hF(z^{-1}) \tag{16}$$

where polynomial F is a tuning parameter that allows to modify the type of closed-loop transfer function: third, second and first order closed-loop system. If the choice of a second order is done, $F(z^{-1})$ is a 1st order polynomial equal to $(1 - z_1 z^{-1})$. Therefore, T is equal to

$$T(z^{-1}) = \frac{(r_0+r_1)}{(1-z_1)}(1 - z_1 z^{-1})$$

The poles of the closed-loop are specified according to the desired response time t_r such as $\omega_0 t_r = 4{,}8$ with $\xi = 1$. More details about the design of polynomial RST are available in [12]-[13].

B. RST with polynomial reference signals

The RST with polynomial reference signals is not totally different from the regular one, but proposes another way to determinate polynomial $T(z^{-1})$ in order to eliminate the steady state errors, for example in response to a ramp reference [20].

To understand the approach some point need to be specified. The open loop transfer function is defined as:

$$H(z^{-1}) = \frac{B(z^{-1})}{A(z^{-1})} = \frac{B^- B^+}{A^- A^+} \tag{17}$$

where B^- and A^-contain all the unstable and extra zeros and pure delays of the plant, which are not compensated. B^+ and

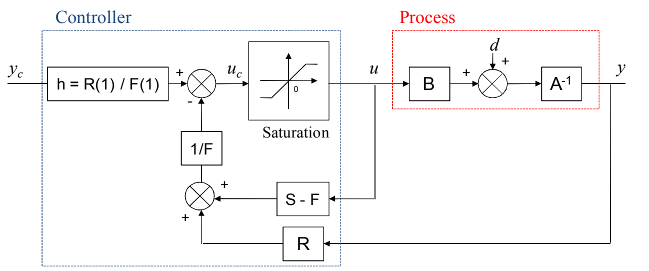

Fig. 4. System with RST anti-windup controller.

A^+ contain all the other terms. In our case, A^-, A^+, B^- and B^+ are defined as follows:

$$A^- = 1 - az^{-1}$$
$$A^+ = 1$$
$$B^- = z^{-1}$$
$$B^+ = K(1-a)$$

To design the controller by pole placement, a transfer model of the closed-loop system is searched from the following expression:

$$F_m(z^{-1}) = \frac{B_m(z^{-1})}{A_m(z^{-1})} \quad (18)$$

The closed-loop transfer function is defined as:

$$\frac{y(z^{-1})}{y_c(z^{-1})} = \frac{BT}{AS+BR} \quad (19)$$

then, the equality between Equ. (18) and Equ. (19) must be performed. $F_m(z^{-1})$ is chosen arbitrarily in order to impose the desired closed loop poles. But with the constraint that $B_m(z^{-1})$ has to contain as a factor, the pure delay of the system, its unstable zeros (uncompensable) and zeros that the designer decides not to compensate, i.e. $B^-(z^{-1})$.

$$B_m = B^- B'_m \quad (20)$$

According to Equ. (18), the partial transfer function from reference y_c to true error signal $\varepsilon(z^{-1}) = y_c(z^{-1}) - y(z^{-1})$ is given by:

$$\frac{\varepsilon(z^{-1})}{y_c(z^{-1})} = 1 - F_m(z^{-1}) = \frac{A_m - B_m}{A_m} \quad (21)$$

In order to cancel steady state errors in response to a ramp reference $y_c(t) = t^m$, . The corresponding z transform is:

$$y_c(z^{-1}) = \frac{y_{c1}}{(1-z^{-1})^{m+1}}$$

where y_{c1} is some polynomial in z^{-1}. m is equal to 1 in this example. It is necessary and sufficient that $(1-z^{-1})^{m+1}$ divides $A_m - B_m$, the following equation must be solved:

$$(1-z^{-1})^{m+1} L + B^- B'_m = A_m \quad (22)$$

This equation is called auxiliary Diophantine equation in [20]. $L(z^{-1})$ is an unknown polynomial, to be determined, and its order is a tuning parameter. The closed-loop system is a second order:

$$A_m = 1 - 2e^{-\xi\omega_0 T_s}\cos(\omega_p T_s)\, z^{-1} + e^{-\xi\omega_0 T_s} z^{-2} \quad (23)$$

with $\omega_p = \sqrt{1-\xi^2}$. Polynomials $L(z^{-1})$ and $B'_m(z^{-1})$ become solutions to Equ. (22), and tuning parameters L and B'_m are defined as:

$$L(z^{-1}) = l_0 + l_1 z^{-1}$$
$$B'_m(z^{-1}) = b'_0 + b'_1 z^{-1}$$

The resolution of Equ. (21) gives:

$$b'_0 = 2e^{-\xi\omega_0 T_s}\cos(\omega_p T_s) - 2$$
$$b'_1 = e^{-\xi\omega_{n0} T_s} - 1$$
$$l_0 = 1$$
$$l_1 = 0$$

Moreover, another constraint is imposed in order to ensure a unity gain in steady state. A constant factor A_0 is introduced to make $F_m(1) = 1$, i.e.:

$$T = A_0 B'_m \quad (24)$$

where the filter polynomial A_0 is often set equal to one [20]. From Eq. (22), polynomials L and B'_m are identified, so polynomial T is known. The determination of polynomial R and S defined in the previous section are still available.

C. RST with sinusoidal reference signals

The RST with sinusoidal references is quiet similar to the RST with polynomial references, except for the expression of the transfer function ε/y_c. Its magnitude is:

$$\left|\frac{\varepsilon(z^{-1})}{y_c(z^{-1})}\right|_{z=e^{j\omega T_s}} = \left|\frac{A_m - B_m}{A_m}\right|_{z=e^{j\omega T_s}} \quad (25)$$

In order to cancel the error at a given angular frequency ω_s, it is necessary to introduce a zero transmission into the transfer function for this frequency. For that, the product $(1 - e^{j\omega_s T_s} z^{-1})(1 - e^{-j\omega_s T_s} z^{-1})$ divides $A_m - B_m$. From this, the auxiliary Diophantine equation is defined as [13]:

$$(1 - 2cos\omega_s T_s z^{-1} + z^{-2})L + B^- B'_m = A_m \quad (26)$$

Like in the previous section, A_m is chosen equal to a second order polynomial. Its discrete expression is given by Eq. (23). The auxiliary Diophantine equation Eq. (26) allows to identify polynomials $L(z^{-1})$ and $B'_m(z^{-1})$:

$$L(z^{-1}) = 1$$
$$B'_m(z^{-1}) = b'_0 + b'_1 z^{-1}$$

with

$$b'_0 = 2e^{-\xi\omega_0 T_s}\cos(\omega_p T_s) + 2cos\omega_s T_s$$
$$b'_1 = e^{-\xi\omega_{n0} T_s} - 1$$

$T(z^{-1})$ is obtained from Eq. (24), $R(z^{-1})$ and $S(z^{-1})$ by the resolution of the regular Diophantine equation Eq. (14).

IV. PERFORMANCES OF THE CONTROLLERS

The different RST controllers are implemented to regulate the currents absorbed by the power converter to the mains. As mentioned in section II, by neglecting the mutual inductances and compensating disturbances, the single-phase PFC converter is equivalent to 5 independents first order transfer functions. Fig. 5 shows the control block diagram of the system. The external loop is the voltage loop; the controller

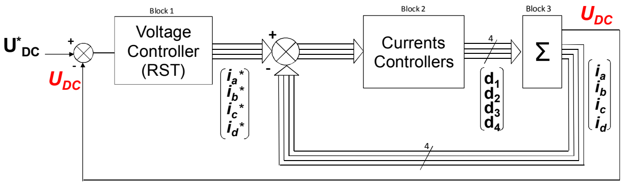

Fig. 5. Control block diagram.

used to regulate the DC link voltage is a regular RST. The inner loops represent the currents loops.

Simulations have been done for each RST controller based on the following parameters:

TABLE I
SIMULATION PARAMETERS

Vgrid	RMS grid voltage (V)	240
$U_{dc}ref$	DC link reference voltage (V)	400
V_{cm}	Common mode voltage (V)	$U_{dc}ref$ / 2
rload	Load resistance (Ω)	53,3
Rs	Stator resistances (Ω)	0,33
P	Output power (kW)	3,3
T_{ri}	Current loops response time (ms)	0,8
T_{ro}	Voltage loop response time (ms)	16
L_{mean}	Mean value of the inductance (mH)	3,3
θ	Mechanical rotor position (°)	22

Fig. 6 shows DC link voltage U_{dc} and winding current i_a obtained for each controller. In Fig. 6.a, the relative error between the reference and the signal is bigger than in the other cases. Indeed for ramp and sinus references, the static error is 10 times less important. For this application, there are no significant differences between RST with ramp reference and RST with sinusoidal one. This can be explained because the frequency of the signal used as reference is low. Therefore, the two types of controllers can be used. These controllers provide a better accuracy compare to the regular RST. For such controllers, the phase shift between the grid voltage and the grid current is very small. For the regular RST controller, the resulting power factor is 0.98 against 1 for the two other RST controllers. In table II, the current spectra i_s (grid current) are compared to standard specifications given in IEC 1000-3-2. For each controller the current harmonics are under the required limits.

TABLE II
HARMONIC CURRENT

Harmonic Order (n)	*Standard IEC 1000-3-2 (A)*	*Result for 3kW (A)*		
		Regular RST	*RST with ramp ref.*	*RST with sinus ref.*
1		18.46	18.37	18.37
2	1.08	0.01	0.01	0.01
3	2.3	0.37	0.41	0.40
4	0.43	0.30	0.30	0.30
5	1.44	0.01	0.01	0.01
6	0.30	0.92×10^{-3}	1.4×10^{-3}	1.4×10^{-3}
7	0.77	0.51×10^{-3}	1.1×10^{-3}	1.1×10^{-3}
8	0.27	0.98×10^{-3}	1.1×10^{-3}	1.1×10^{-3}
9	0.40	0.89×10^{-3}	0.93×10^{-3}	0.93×10^{-3}
10	0.27	0.78×10^{-3}	0.89×10^{-3}	0.89×10^{-3}

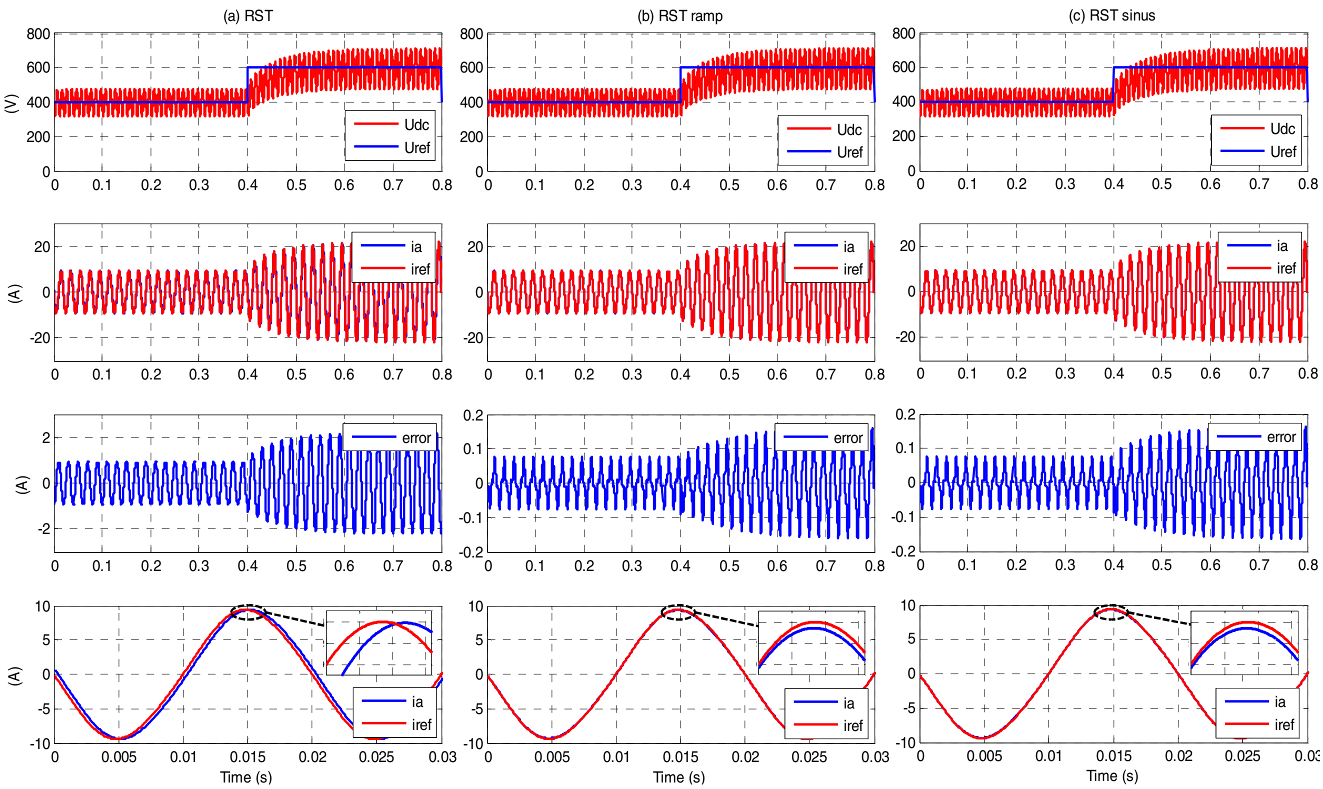

Fig. 6. Voltage and current regulation of single phase PWM for 3 kinds of RST controllers.

Some robustness tests were done in order to compare the controllers from this particular point of view. Fig. 7 shows the current control for inductances disturbances and stator resistances disturbances of $\pm 50\%$. For these variations, there is no influence on the current control. The RST presented here are all robust. Moreover, the computation gain is better in RST with ramp and sinus references case: $2e^6$ against $2.4e^6$ for the classical one.

V. Conclusion

This paper has presented three RST controllers designed to control currents in the single-phase battery charger of an Electric Vehicle. The power converter structure and its particularities have been pointed out. The design of the controllers has been described and a comparison between them has been done.

Simulations results on the single-phase PWM rectifier have shown that better performances can be obtained for RST calculated with ramp and sinusoidal references. RST designed for ramp and sine wave references present more accuracy than the regular RST. The robustness is guaranteed whatever the chosen RST, this is due to the robust poles placement. Moreover the computation of these controllers is simple.

Acknowledgment

This work was supported by the French automotive cluster MOVEO in a FUI program, through the project SOFRACI.

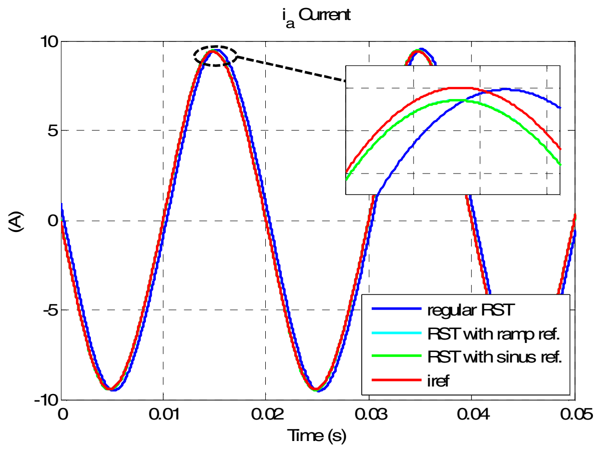

Fig. 7. Robustness test with 50% of parameters variations on current control for 3 RST controllers.

References

[1] P. Bastard, *"Key issues for Electric Vehicles mass market development"*. International Conference and Exhibition on Automotive Power Electronics (APE) proceedings, France, April 2011.

[2] L. Solero, *"Nonconventional on-board charger for electric vehicle propulsion batteries"*. IEEE Transactions on Vehicular Technology, vol. 50, no. 1, pp. 144-149, January 2001

[3] L. Shi, A. Meintz, M. Ferdowsi, *"Single-phase bidirectional AC-DC converters for plug-in hybrid electric vehicle applications"*. IEEE Vehicle Power and Propulsion Conference (VPPC), Harbin, China, September 2008.

[4] S. K. Sul, S. J. Lee, *"An integral battery charger for four-wheel drive electric vehicle"*. IEEE Transactions on Industry Applications, vol. 31, no. 5, pp. 1096-1099, September 1995.

[5] S. Haghbin, K. Khan, S. Lundmark, M. Alakula, O. Carlson, M. Leksell, O. Wallmark, *"Integrated chargers for EVs and PHEVs: Example and new solutions"*. International Conference on Electrical Machines (ICEM) proceedings, Italy, September 2010.

[6] S. Haghbin, M. Alakula, K. Khan, S. Lundmark, M. Leksell, O. Wallmark, O. Carlson, *"An integrated charger for plug-in hybrid electric vehicles based on a special interior permanent magnet motor"*. IEEE Vehicle Power Propulsion Conference (VPPC), France, September 2010.

[7] L. De Sousa, B. Silvestre, B. Bouchez, *"A combined multiphase electric drive and fast battery charger for electric vehicles"*. IEEE Vehicle Power Propulsion Conference (VPPC), France, September 2010.

[8] B. Bouchez, L. De Sousa, *"Rethink the Electrical Vehicle architecture"*, International Conference and Exhibition on Automotive Power Electronics (APE) proceedings, France, April 2011.

[9] A. Bruyère, L. De-Sousa, B. Bouchez, P.Sandulescu, X. Kestelyn, E. Semail, *"A multiphase traction /fast –battery-charger drive for electric or plug-in hybrid vehicles"*. IEEE Vehicle Power Propulsion Conference (VPPC), France, September 2010.

[10] L. De Sousa, B. Bouchez, J. L. Da Costa, *"A new on-board fast battery charger"*. International Conference and Exhibition on Automotive Power Electronics (APE) proceedings, France, April 2011.

[11] S. Lacroix, E. Labouré, M. Hilairet, *"An integrated fast battery charger for electric vehicle"* IEEE Vehicle Power Propulsion Conference (VPPC), France, September 2010.

[12] P. De Larminat, *"Automatique – Commande des systèmes linéaires"*. 2nd edition, Hermès, Paris, pp. 177-187, 1998.

[13] E. Ostertag, E. Godoy, *"RST-Controller design for sinewave references by means of an auxiliary Diophantine equation"*. Proceedings of the 44th IEEE Conference on Decision and Control, and the European Control Conference, Spain, December 2005.

[14] F. Poitiers, T. Bouaouiche, M. Machmoum, *"Advanced control of a doubly-fed induction generator for wind energy conversion"*. Electric Power Systems Research, vol. 79, pp. 1085-1096, 2009.

[15] F. Mekri, M. Machmoum, N. Aït-Ahmed, B. Mazari, *"A comparative study of voltage controllers for series active power filter"*. Electric Power Systems Research, vol. 80, pp. 615-626, 2010.

[16] F. J. Carillo, F. Rotella, *"A robust adaptative controller for constant turning force regulation"*. Control Eng. Practice, vol. 5, no. 12, pp. 1673-1682, 1997.

[17] X. Lin-Shi, B. Allard, D. Tournier, J. M. Rétif, F. Morel *"A digital-controller parameter-tuning approach, application to a switch-mode power supply"*. IEEE International Symposium on Industrial Electronics (ISIE), pp. 3356-3361, Vigo, Spain, June 2007.

[18] R. N. Andriamalala, H. Razik, F.M. Sargos *"Indirect-Rotor-Field-Oriented-Control of a Double-Star Induction Machine Using the RST Controller"*. 34th Annual Conference of the IEEE Industrial Electronics (IECON), pp.3108 -3113, Orlando, January 2008.

[19] X. Lin-Shi, B. Allard, D. Tournier, J. M. Rétif, F. Morel, *"Digital control strategies for switch-mode power supply"*. 32nd Annual Conference on IEEE Industrial Electronics (IECON), pp. 79-84, Paris, France, November 2006.

[20] E. Ostertag, *"Steady-state error-free RST-controller design: a double Diophantine equation approach"*. Proc. 5th European Control Conference (ECC), Karlsruhe, Germany, 1999.

[21] E. Godoy, E. Ostertag, *"A complete methodology for the design of a digital control law for PWM inverters"*. 10th European Conference on Power Electronics and Applications (EPE), Toulouse, France, 2003.